

Article

Antimicrobial Activity and Mode of Action of Celastrol, a Nortriterpen Quinone Isolated from Natural Sources

Nayely Padilla-Montaño, Leandro de León Guerra  and Laila Moujir * 

Departamento de Bioquímica, Microbiología, Biología Celular y Genética, Facultad de Farmacia, Universidad de La Laguna, Avenida Astrofísico Fco Sánchez s/n, 382016 Tenerife, Spain; nayelypadilla@hotmail.com (N.P.-M.); lleongue@ull.edu.es (L.d.L.G.)

* Correspondence: lmoujir@ull.edu.es; Tel.: +34-922-318-513

Abstract: Species of the Celastraceae family are traditionally consumed in different world regions for their stimulating properties. Celastrol, a triterpene methylene quinone isolated from plants of celastraceas, specifically activates satiety centers in the brain that play an important role in controlling body weight. In this work, the antimicrobial activity and mechanism of action of celastrol and a natural derivative, pristimerin, were investigated in *Bacillus subtilis*. Celastrol showed a higher antimicrobial activity compared with pristimerin, being active against Gram-positive bacteria with minimum inhibitory concentrations (MICs) that ranged between 0.16 and 2.5 µg/mL. Killing curves displayed a bactericidal effect that was dependent on the inoculum size. Monitoring of macromolecular synthesis in bacterial populations treated with these compounds revealed inhibition in the incorporation of all radiolabeled precursors, but not simultaneously. Celastrol at 3 µg/mL and pristimerin at 10 µg/mL affected DNA and RNA synthesis first, followed by protein synthesis, although the inhibitory action on the uptake of radiolabeled precursors was more dramatic with celastrol. This compound also caused cytoplasmic membrane disruption observed by potassium leakage and formation of mesosome-like structures. The inhibition of oxygen consumption of whole and disrupted cells after treatments with both quinones indicates damage in the cellular structure, suggesting the cytoplasmic membrane as a potential target. These findings indicate that celastrol could be considered as an interesting alternative to control outbreaks caused by spore-forming bacteria.

Keywords: celastrol; Celastraceae; antimicrobial activity; mechanism of action; *Bacillus subtilis*



Citation: Padilla-Montaño, N.; de León Guerra, L.; Moujir, L. Antimicrobial Activity and Mode of Action of Celastrol, a Nortriterpen Quinone Isolated from Natural Sources. *Foods* **2021**, *10*, 591. <https://doi.org/10.3390/foods10030591>

Academic Editors: Ana Maria Loureiro da Seca and Antoaneta Trendafilova

Received: 12 February 2021
Accepted: 5 March 2021
Published: 11 March 2021

Publisher's Note: MDPI stays neutral with regard to jurisdictional claims in published maps and institutional affiliations.



Copyright: © 2021 by the authors. Licensee MDPI, Basel, Switzerland. This article is an open access article distributed under the terms and conditions of the Creative Commons Attribution (CC BY) license (<https://creativecommons.org/licenses/by/4.0/>).

1. Introduction

Historically, plants have provided a wide variety of active compounds, becoming a key element in the development of many cultures. The Celastraceae family, commonly known as the bittersweet family, comprises a group of plants distributed mainly in tropical and subtropical regions of the world including North Africa, South America, and East Asia. It has a long history in traditional medicine as a stimulant, diuretic, emmenagogue, anti-inflammatory, antibacterial, anti-cancer, and for the treatment of gastrointestinal disorders among others [1]. In the Canary Islands, East Africa, and the Arabian Peninsula, the leaves of members of this family are chewed to combat fatigue [1,2]. In our search for antimicrobial compounds from plants, we isolated celastrol and its methylated derivative, pristimerin, which are the first and the most frequently reported celastroloids. The term celastroloid refers to methylene quinone nor-triterpenes with a 24-nor-D: A-friedo-oleanane skeleton, which, later on, was extended to related phenolic nor-triterpenes [3] and their dimer and trimer congeners. The two natural pentacyclic triterpenoids celastrol and pristimerin are commonly found in the roots and bark of Celastraceae species. Both compounds show a wide range of pharmacological activities, including anti-cancer, anti-inflammatory, antioxidant, hepatoprotective, or immunomodulatory, among others [4–8]. The anti-cancer properties of celastrol, one of the most studied methylene quinones, have been attributed

to apoptosis and autophagy induction, cell cycle arrest, and anti-metastatic and anti-angiogenic action [9,10]. Other works have evidenced the ability of celastrol in combating metabolic disorders such as obesity and type 2 diabetes [11]. Treatment with celastrol suppresses food intake, blocks reduction in energy consumption, and mediates weight loss by acting as a leptin sensitizer in mouse models [12,13].

In addition to these pharmacological activities, antimicrobial properties have also been demonstrated for these and other related triterpenoids such as tingenone, netzahualcoyone, or zeylasterone that exhibit inhibitory activity against Gram-positive bacteria [14–17]. Moreover, the anti-biofilm [18–20] and anti-fouling properties of celastrol and pristimerin have been reported on a wide variety of microorganisms [21], as well as anti-mycotic activity [22–27]. Besides, celastrol and its derivatives have also shown inhibitory activity against viruses producing hepatitis B and C [28,29], which makes them potentially useful compounds for the control of various diseases. This paper describes the antimicrobial activity and mechanism of action of celastrol and pristimerin using *Bacillus subtilis* as a model of spore-forming bacteria. Species of *Bacillus* have been associated with many food contaminations causing food-borne illness in humans [30], spoilage of processed food products [31,32], or certain pathologies such as pneumonia, bacteremia, and meningitis in immunosuppressed patients [33–35]. Regardless of variations in disease presentation, the etiologic agent is often the spore and the production of toxins that play a central role in the pathophysiology of the infection. Although it is generally accepted that the antimicrobial activity of terpenoid compounds involves damage on plasma membrane [36], little is known about how this affects other cellular processes essential to bacterial cell development. Thus, the action of these compounds on different metabolic pathways such as macromolecular synthesis, uptake of solutes and biosynthetic precursors, or the damage on membrane function was investigated.

2. Materials and Methods

2.1. Microorganisms

Strains used for determining antimicrobial activity included *Bacillus subtilis* ATCC 6051, *B. cereus* ATCC 21772, *B. megaterium* ATCC 25848, *B. pumilus* ATCC 7061, *Staphylococcus aureus* ATCC 6538, *S. epidermidis* ATCC 14990, *S. saprophyticus* ATCC 15305, *Enterococcus faecalis* CECT 795 (from Type Culture Spanish Collection), *Mycobacterium smegmatis* ATCC 19420, *Proteus mirabilis* CECT170, *Escherichia coli* ATCC 9637, *Pseudomonas aeruginosa* AK958 (from the University of British Columbia, Department of Microbiology collection), *Salmonella* spp. CECT 456, and *Candida albicans* CECT 1039.

Bacterial cultures were developed at 37 °C in nutrient broth (NB), except for *E. faecalis* and *M. smegmatis* that were grown in brain heart infusion broth (BHI), or *C. albicans* cultured in Sabouraud liquid medium. All media were purchased from Oxoid.

2.2. Quinones and Others Antibacterial Compounds

Celastrol and pristimerin were isolated, purified, and characterized from the roots of Celastraceae species as previously reported [37,38]. Pure compounds were dissolved in dimethyl sulfoxide (DMSO) before the evaluation. The reference antibacterial agents ciprofloxacin, rifampicin, tetracycline, penicillin, and clofoctol (Sigma-Aldrich, St. Louis, MO, USA) were used as controls according to the Clinical and Laboratory Standards Institute [39].

2.3. Determination of Minimum Inhibitory Concentration (MIC) and Minimum Bactericidal Concentration (MBC)

The antimicrobial activity was determined for each compound in triplicate by broth microdilution method (range 0.08–40 µg/mL) in 96-well microtiter plates, according to the M07-A9 approved standard of the Clinical and Laboratory Standards Institute (CLSI) [40]. Wells with the same proportions of DMSO were used as controls and never exceeded 1% (v/v). The starting concentration of microorganism ranged between 1 and 5×10^5 colony-forming

units (CFU)/mL, and growth was monitored by measuring the increase in optical density at 550 nm (OD_{550}) with a microplate reader (Infinite M200, Tecan Group Ltd., Männedorf, Switzerland) and viable count in agar plates. The minimum inhibitory concentration (MIC) was defined as the lowest concentration of compound that completely inhibits growth of the organisms compared to the untreated cells. All wells with no visible growth were subcultured in duplicate by transferring (100 μ L) to nutrient, BHI, or Sabouraud agar plates. After overnight incubation, colony counts were performed and the minimum bactericidal concentration (MBC) was defined as the lowest compound concentration that produces $\geq 99.9\%$ killing of the initial inoculum.

2.4. Bacterial Killing Assays

Overnight liquid cultures of *B. subtilis* were diluted in Monod's flask containing 10 mL of NB medium, to give a working concentration ranging between 1 and 5×10^5 CFU/mL. Celastrol (3 μ g/mL) or pristimerin (10 μ g/mL) was added at time 0 (lag phase) or after 3 h of incubation (log-phase, $OD_{550} \approx 0.4$). These suspensions were incubated at 37 °C in a rotator shaker and growth was monitored by measuring the OD_{550} and CFU count on nutrient agar plates. Cultures with known antibiotics or without drugs were used as positive and negative controls, respectively. The assays were repeated at least three times.

2.5. Inoculum Effect

Overnight liquid cultures of *B. subtilis* were 10-fold serial diluted in NB medium to give different inoculum concentrations (10^3 to 10^7 CFU/mL). Celastrol (3 μ g/mL) and pristimerin (10 μ g/mL) were added and cultures were incubated at 37 °C in a rotatory shaker. Bacterial growth was monitored as described above. The assays were repeated at least three times.

2.6. Measurement of Radioactive Precursor Incorporation

Cultures of *B. subtilis* were diluted to obtain 10^6 CFU/mL in Davis–Mingoli medium [41] supplemented with glucose (1%), asparagine (0.1 g/L), and casamino acids (2 g/L) (pH 7). The cultures were grown at 37 °C under shaking for at least 3 h to obtain an optical density (OD_{550}) of 0.4. Volumes of 10 mL were transferred to prewarmed flasks containing celastrol (3 μ g/mL) or pristimerin (10 μ g/mL) and one of the precursors of DNA (1 μ Ci/mL [$6\text{-}^3\text{H}$] + 2 μ g/mL unlabeled thymidine), RNA (1 μ Ci/mL [$5\text{-}^3\text{H}$] + 2 μ g/mL unlabeled uridine), protein (5 μ Ci/mL [$4,5\text{-}^3\text{H}$] + 2 μ g/mL unlabeled leucine), or cell wall peptidoglycan (0.1 μ Ci/mL *N*-Acetyl-D-[$1\text{-}^{14}\text{C}$] glucosamine). The samples were incubated at 37 °C under shaking. Volumes of 0.5 mL were collected and precipitated with 2 mL ice-cold 10% trichloroacetic acid (TCA) at different times. After 30 min of incubation in cold TCA, samples were filtered on glass microfiber filters grade GF/C (Whatman, Maidstone, UK) and washed three times with 5 mL cold 10% TCA and once with 5 mL of 95% ethanol. The dried filters were placed in vials covered with a scintillation cocktail and counted in counter LKB Wallac Rackbeta (Perkin Elmer, Courtaboeuf, France). Macromolecular synthesis was measured by quantifying the incorporation of radiolabeled precursors (Amersham Biosciences Europe GmbH) into acid-insoluble material. Evaluations with DMSO added in the same proportion or a specific inhibitor of each biosynthetic pathway were included as negative and positive controls, respectively.

2.7. Measurement of Solutes Uptake

Solute uptake was measured as total cell-associated counts after addition of quinones on cultures of *B. subtilis* growing exponentially ($OD_{550} \approx 0.2$). Growing cells containing half concentration of NB medium were transferred to prewarmed flasks containing celastrol (3 μ g/mL) or pristimerin (10 μ g/mL) and radiolabeled glucose (2 μ Ci/mL D-[$1\text{-}^{14}\text{C}$]-glucose) or the precursors of DNA, RNA, protein, and cell wall peptidoglycan (see concentrations in previous section). At different times (up to 30 min), 0.5 mL of samples was collected and filtered through Millipore filters of 0.45- μ m pore size (Type HA, Mil-

lipore Corporation, Burlington, MA, USA). Filters were washed three times with 5 mL phosphate buffer, dried, and radioactivity was measured as above. Samples with clofoctol (5 µg/mL) or DMSO at the same concentration were included as positive and negative controls, respectively.

Furthermore, the effect of celastrol on the uptake and incorporation of radiolabeled precursors of DNA was also evaluated when the macromolecular synthesis was inhibited. *B. subtilis* cultures prepared as described above were treated for 30 min with the specific inhibitor ciprofloxacin (1.5 µg/mL) before the addition of labeled and unlabeled precursor. After 5 min, celastrol (3 µg/mL) or the same proportion of DMSO in control cultures was incorporated. At different times, precursor uptake and incorporation was measured as mentioned above. The assays were repeated at least three times.

2.8. Inhibition of DNA Gyrase

Inhibition of DNA gyrase was performed using the Gyrase Supercoiling kit 1 (#K001) (John Innes Enterprises Ltd., Norwich, UK) as described in the manufacturer's instructions. Two units of DNA gyrase were incubated with 0.5 µg relaxed plasmid pBR322 and 50 µg/mL of celastrol or pristimerin in a final volume of 30 µL. Ciprofloxacin at 25 and 50 µg/mL was used as positive control. The samples were incubated at 30 °C for 30 min and the products were visualized in 0.8% agarose gel containing 0.5 µg/mL ethidium bromide.

2.9. Integrity of Cell Membrane

Bacterial membrane damage was examined by determination of the release of material absorbing at 260/280 nm, detection of potassium (K⁺) leakage, and the BacLight Live/Dead staining method (Invitrogen Molecular Probes, Eugene, OR, US). *B. subtilis* cultures in log-phase growth (OD₅₅₀ ≈ 0.8) were centrifuged at 15,000 × *g* for 10 min at 4 °C and washed twice with saline buffer. The pellet was resuspended in the same buffer to obtain a bacterial concentration of 1–2 × 10⁸ CFU/mL (or 1–2 × 10⁷ CFU/mL for K⁺ leakage experiments). Cell cultures were treated with celastrol (3 µg/mL) and incubated at 37 °C under shaking. Cultures with clofoctol (10 µg/mL) or DMSO at the same concentration were used as positive and negative controls, respectively. Samples were collected for quantification at different times over a 30-min period. Liberation of cytoplasmic materials was monitored by measuring the optical density (OD₂₆₀ and OD₂₈₀) of the supernatant after removing cells by centrifugation (at 9500 × *g* for 10 min, 4 °C) or after membrane filtration by means of an atomic absorption spectrophotometer (Model Thermo S-Series, Thermo Electron Corporation, Cambridge, UK) for K⁺ release. The BacLight assay was analyzed after a 20-min dark-staining period following the manufacturer's instructions. The cells were visualized at ×1000 magnification with an epifluorescence microscope (Leica DM4B, Leica Microsystems GmbH, Wetzlar, Germany) provided with a fluorescein–rhodamine dual filter.

2.10. Transmission Electron Microscopy

To further confirm the mode of action of celastrol on *B. subtilis*, transmission electron microscopy (TEM) analysis was performed. Suspensions of *B. subtilis* in log-phase growth (10⁷ CFU/mL) were treated with celastrol (3 µg/mL) for 1 h at 37 °C and were harvested at 6500 × *g* for 8 min at 4 °C. For comparative purposes, bacterial cells grown under the same conditions were also treated with pristimerin (10 µg/mL). Subsequently, bacteria were washed in fixative buffer, post-fixed in 1% osmium tetroxide in fixative buffer, and washed with distilled water. Sections (1 µm) were cut with a Reichert Ultracut ultramicrotome and stained with toluidine blue; ultra-thin sections were contrasted with uranyl acetate and lead. Preparations were observed under a Zeiss EM 912 transmission electron microscope. Images were captured with a Proscan Slow-scan CCD-Camera for TEM (Proscan, Scheuring, Germany) and Soft Imaging System software (version 5.2, Olympus Soft Imaging Solutions GmbH, Münster, Germany). Control experiments with the same proportion of DMSO were performed in parallel.

2.11. Oxygen Consumption

Suspensions of *B. subtilis* and *E. coli* in the log phase of growth ($OD_{550} \approx 0.8$) were centrifuged at $15,000 \times g$ for 10 min at 4 °C and washed twice with phosphate buffer 0.1 M (pH 7.0). Then, the pellet was suspended in the same buffer to obtain a bacterial concentration of $1\text{--}2 \times 10^7$ CFU/mL. Cells suspensions (2.7 mL) supplemented with 0.3 mL of 10% glucose were used to measure oxygen consumption at room temperature in a glass cell of Clark oxygen electrode equipped with a magnetic stirrer. Celastrol (at 3 µg/mL for *B. subtilis* and 20 µg/mL for *E. coli*) was added to the cell suspension, and the steady-state output of the oxygen electrode (after 4 min) was measured using a digital biological oxygen monitor (model YSI 5300, Yellow Springs, OH, USA). DMSO in the same proportion and sodium cyanate at 6.7 mM were used as negative and positive controls, respectively. Furthermore, disrupted cell preparations of *B. subtilis* and *E. coli* were used to determine the effect of celastrol on oxygen uptake using NADH (0.1 mM) as a substrate. Cultures grown in yeast extract and peptone (YP, 1% *w/v*) medium for 18 h at 37 °C under aeration were collected by centrifugation at $10,000 \times g$ for 10 min at 4 °C. Cells were washed twice in 0.1 M potassium phosphate buffer (pH 7.0), resuspended in the same buffer (5 mL of buffer per gram of cells), and sonicated (Labsonic M, Sartorius Stedim Biotech, Göttingen, Germany) for 15 min in 10-s bursts with 20-s stop intervals. Intact cells were removed by centrifugation at $4000 \times g$ for 10 min at 4 °C. The supernatant was centrifuged at $15,000 \times g$ for 10 min at 4 °C and the pellet was resuspended in the same buffer as before (5 mL). Aliquots (0.2 mL) of disrupted cells were incubated at room temperature in the same buffer (2.8 mL) containing NADH (0.1 mM).

2.12. Statistical Analysis

Three independent experiments were conducted for each evaluation and means and standard deviations (\pm SD) were calculated. Analysis of variance (one-way ANOVA) followed by Tukey's multiple comparison test ($p < 0.05$) to extract the specific differences between treatments were performed using R statistical software environment version 4.0.3 (R Foundation for Statistical Computing, Vienna, Austria).

3. Results and Discussion

3.1. Antimicrobial Activity

Table 1 shows the MICs and MBCs of celastrol and pristimerin against different microorganisms used in this study. Celastrol was active against all Gram-positive bacteria evaluated, with MIC values ranging between 0.16 (*B. subtilis*) and 2.5 µg/mL (*S. saprophyticus*). Compared to celastrol, pristimerin showed weaker activity on Gram-positive bacteria and no action on *S. aureus* and *M. smegmatis*. On the basis of these results, *B. subtilis* was selected to evaluate the mechanism of action of these quinones.

Table 1. Minimum inhibitory concentration (MIC)¹ and minimum bactericidal concentration (MBC)¹ of celastrol and pristimerin, expressed in µg/mL against different microorganisms².

Microorganisms	Celastrol		Pristimerin	
	MIC	MBC	MIC	MBC
<i>Bacillus subtilis</i>	0.156	2.5	1.25	10
<i>B. cereus</i>	0.625	2.5	10	>40
<i>B. pumilus</i>	0.625	2.5	2	10
<i>B. megaterium</i>	1.25	5	20	>40
<i>Staphylococcus aureus</i>	1.25	>40	>40	>40
<i>S. epidermidis</i>	0.312	15	1.25	>40
<i>S. saprophyticus</i>	2.5	10	10	10
<i>Mycobacterium smegmatis</i>	5	>40	>40	>40
<i>Enterococcus faecalis</i>	1.25	40	20	>40

¹ Values represent average obtained from a minimum of three experiments. ² The quinone compounds were inactive against Gram-negative bacteria and the yeast assayed (MIC > 40 µg/mL).

Gram-negative bacteria and the yeast *C. albicans* were insensitive to the action of both compounds at the maximum concentration assayed (40 $\mu\text{g}/\text{mL}$). The inactivity of pristimerin against *S. aureus* was previously reported by our group [24], although in later works, da Cruz et al. [42] indicated MIC values of 25 $\mu\text{g}/\text{mL}$. The use of a bacterial strain of *S. aureus* less sensitive to the activity of the compound could explain this difference in the results. Gullo et al. [23] reported antimicrobial activity for pristimerin against *C. albicans* with an MIC of 250 $\mu\text{g}/\text{mL}$. In our evaluations, the maximum concentration tested was 40 $\mu\text{g}/\text{mL}$ since higher concentrations of both compounds led to solubility problems.

These products differ in the functional group in ring E (Figure 1). As previously reported for other methylene quinones and phenolic nor-triterpenes compounds, replacement of the carboxylic group present in celastrol on C-29 by a methyl ester group reduces the antibacterial activity [14,43]. Celastrol has shown interesting pharmacological activities, although inconveniences related to poor water solubility, high toxicity, or poor stability have also been described [29,44]. Structural modifications in the triterpene quinones scaffolds could be of interest to obtain derivatives with improved antimicrobial activities and to overcome the pharmacokinetic limitations of these compounds.

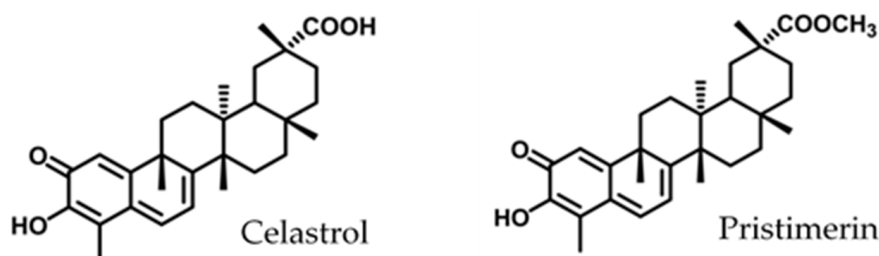


Figure 1. Structure of triterpenoid methylene quinones.

3.2. Effects of Methylene Quinones against *B. subtilis*

The time–kill curves of *B. subtilis* cultures showed a different behavior when celastrol and pristimerin were added at different growth stages (Figure 2). Addition of celastrol at 3 $\mu\text{g}/\text{mL}$ in the lag phase (10^5 CFU/mL) had a bactericidal effect similar to ciprofloxacin with ≥ 3 Log_{10} in CFU reduction after 9 h of incubation (Figure 2A). Rifampicin and tetracycline also had a bactericidal behavior in the first hours of treatment, although the cultures recovered after 24 h of incubation. A bacteriostatic action and regrowth was observed with penicillin. Compared to celastrol, pristimerin at 10 $\mu\text{g}/\text{mL}$ had a bacteriostatic effect, producing a minor reduction in the CFU counts (< 3 Log_{10}). However, when pristimerin was incorporated in the log phase of growth (10^7 CFU/mL), a bactericidal action was observed, reducing the bacterial population 4.2 Log_{10} in 2 h of treatment, with up to 99.9% dead after 24 h of incubation (Figure 2B). In addition, the drop in optical density values (OD_{550}) revealed the bacteriolytic nature of this compound. Under these conditions of growth, celastrol had a bacteriostatic action, similar to that shown by ciprofloxacin, tetracycline, and rifampicin, with a clear regrowth of the culture after 24 h in the presence of rifampicin. Penicillin had a limited effect on the control of *B. subtilis* cells actively growing.

The action of the methylene quinones was also evaluated against different inoculum sizes of *B. subtilis* in lag-phase growth (Table 2). At the higher inoculum concentration (10^7 CFU/mL), celastrol showed a bacteriostatic activity during the exposition time and a lower reduction in CFU/mL compared to the log phase of growth (Figure 2B). A bacteriostatic effect was also observed at 10^6 and 10^5 CFU/mL and bactericide at 10^4 CFU/mL. Pristimerin showed a similar behavior to that obtained with celastrol. However, when this compound was added in the log phase of growth, a bacteriolytic effect was observed within 6 h of treatment (Figure 2B). These results indicate that both quinones show a stronger effect when *B. subtilis* is actively growing.

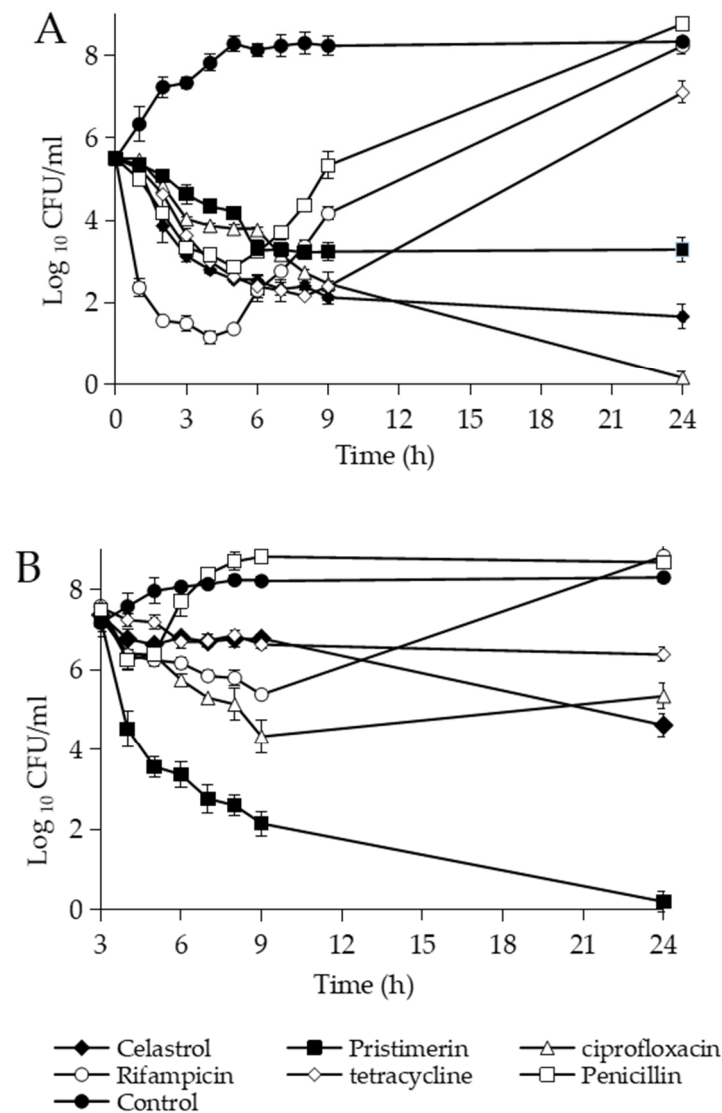


Figure 2. Time–kill curves of *B. subtilis* cultures expressed as Log_{10} of CFU counts after treatment with different antimicrobial substances (celastrol 3 $\mu\text{g}/\text{mL}$; pristimerin 10 $\mu\text{g}/\text{mL}$; ciprofloxacin 1.2 $\mu\text{g}/\text{mL}$; rifampicin 0.15 $\mu\text{g}/\text{mL}$; tetracycline 7.5 $\mu\text{g}/\text{mL}$; and penicillin 9 $\mu\text{g}/\text{mL}$) added in lag phase of growth (A) and log phase after three hours of preincubation (B). Cultures without drugs and with the maximum proportion of DMSO were used as controls. Error bars express SD with $n = 3$.

Table 2. Effect of celastrol at 3 $\mu\text{g}/\text{mL}$ and pristimerin at 10 $\mu\text{g}/\text{mL}$ on different inoculum sizes of *B. subtilis* at 3 and 6 h after treatment.

Triterpene	Dilution Factor	Mean Log_{10} CFU \pm SD ¹		
		Initial Inoculum	Recovery at 3 h	Recovery at 6 h
Celastrol	10 ⁷	7.58 \pm 0.11	7.60 \pm 0.15	7.58 \pm 0.05
	10 ⁶	6.41 \pm 0.14	4.68 \pm 0.27	4.08 \pm 0.17
	10 ⁵	5.54 \pm 0.20	4.00 \pm 0.21	3.15 \pm 0.16
	10 ⁴	4.67 \pm 0.09	2.30 \pm 0.25	1.27 \pm 0.25
Pristimerin	10 ⁷	7.58 \pm 0.12	7.51 \pm 0.07	7.47 \pm 0.05
	10 ⁶	6.35 \pm 0.17	5.32 \pm 0.20	4.71 \pm 0.33
	10 ⁵	5.32 \pm 0.19	4.26 \pm 0.16	3.27 \pm 0.22
	10 ⁴	4.75 \pm 0.11	3.59 \pm 0.12	1.56 \pm 0.10

¹ Data are expressed as mean values \pm standard deviations ($n = 3$).

3.3. Mechanism of Action

3.3.1. Effects of Macromolecular Synthesis and Initial Uptake of Solutes

Initially, the incorporation of radiolabeled precursors into DNA, RNA, protein, and cell wall synthesis was measured. After addition of celastrol and pristimerin, the incorporation of all precursors into the macromolecular synthesis was blocked, but not simultaneously (Figure 3). Celastrol at 3 $\mu\text{g}/\text{mL}$ reduced by $\geq 70\%$ the incorporation of [$6\text{-}^3\text{H}$] thymidine and [$5\text{-}^3\text{H}$] uridine within 5 and 10 min, respectively. The inhibitory effect of celastrol after 5 min was comparable to that observed with the specific inhibitor of the RNA synthesis, rifampicin. Pristimerin at 10 $\mu\text{g}/\text{mL}$ needed at least 30 min to produce an inhibition of 57% and 47% of DNA and RNA synthesis, respectively (Figure 3A,B). Celastrol and pristimerin inhibited the incorporation of leucine into protein synthesis by $>55\%$ after 20 min, whereas tetracycline blocked this process ($>70\%$) in 10 min. The incorporation of *N*-acetyl-D-[^{14}C] glucosamine into peptidoglycan decreased rapidly within 2 min after the addition of celastrol and pristimerin, with inhibition values of 58% and 70%, respectively. However, this effect was not constant over time and the incorporation of the precursor gradually increased after 5 min. Initially, the inhibitory effect produced by penicillin at 30 $\mu\text{g}/\text{mL}$ on cell wall synthesis was slower (32% in 2 min) than with celastrol and pristimerin, but the incorporation of the precursor gradually increased this up to 85% in 30 min (Figure 3D). Clofoctol, a cytoplasmic membrane disruptor [45], had a variable effect on the incorporation of precursors but blocked all biosynthetic processes ($>70\%$ of inhibition) after 30 min of evaluation.

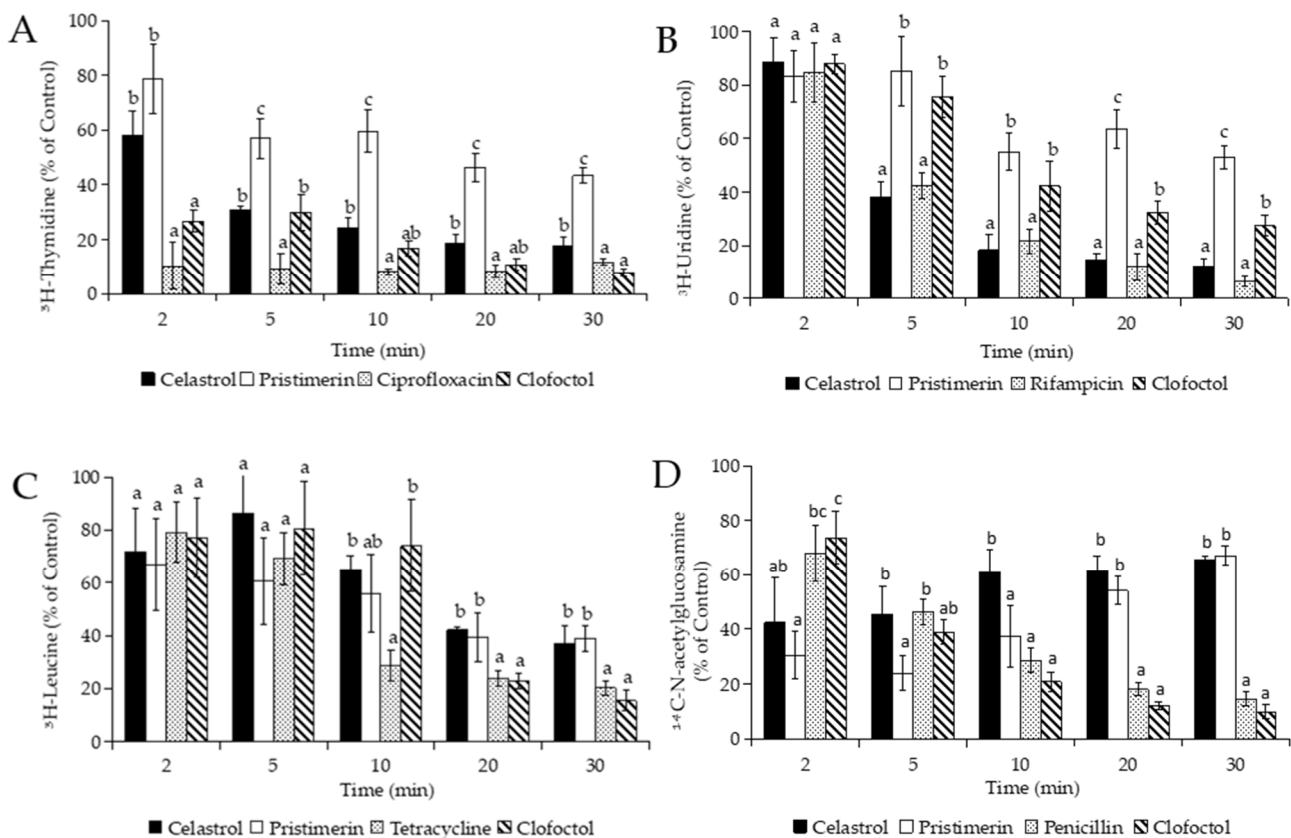


Figure 3. Incorporation of precursor in the synthesis of DNA (A), RNA (B), protein (C), and cell wall (D) of *B. subtilis* cultures in the presence of triterpene methylene quinones (celastrol 3 $\mu\text{g}/\text{mL}$; pristimerin 10 $\mu\text{g}/\text{mL}$), specific inhibitors of each pathway (ciprofloxacin 1.25 $\mu\text{g}/\text{mL}$; rifampicin 0.2 $\mu\text{g}/\text{mL}$; tetracycline 10 $\mu\text{g}/\text{mL}$; and penicillin 30 $\mu\text{g}/\text{mL}$), and clofoctol (5 $\mu\text{g}/\text{mL}$). Data are expressed as percentage (%) of precursors' incorporation compared to controls without drugs but with the maximum proportion of DMSO. Error bars express SD with $n = 3$. Different letters above bars mean significant differences between treated cultures ($p < 0.05$, one-way ANOVA; Tukey's test).

The inhibition of all processes of macromolecular synthesis is more compatible with an indirect effect on biosynthetic pathways rather than a specific action on specific targets [46,47]. Thus, the inhibition produced by celastrol and pristimerin on macromolecular synthesis could be related with damage on the cytoplasmic membrane, as it happens with clofoctol. For this reason, we firstly determined the effect of both compounds on the uptake of glucose by *B. subtilis*, measured as total cell-associated counts after cell isolation from free labeled precursors in the incubation medium. As shown in Figure 4, celastrol at 3 $\mu\text{g}/\text{mL}$ drastically reduced (>70%) the uptake of D-[1- ^{14}C]-glucose in only 2 min, whereas clofoctol needed at least 5 min to produce comparable reductions. Pristimerin weakly reduced the uptake of glucose and required up to 20 min to produce $\approx 50\%$ inhibition.

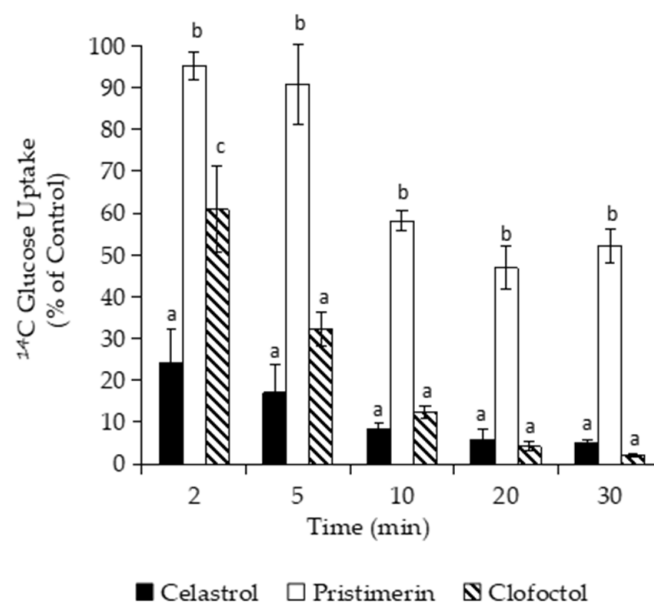


Figure 4. Glucose uptake assay on *B. subtilis* cultures after the addition of the quinones celastrol (3 $\mu\text{g}/\text{mL}$) and pristimerin (10 $\mu\text{g}/\text{mL}$). Clofoctol (5 $\mu\text{g}/\text{mL}$), a known inhibitor of macromolecule uptake, was added as a positive control. Data are expressed as percentage (%) of precursor incorporation compared to controls without drugs but with the maximum proportion of DMSO. Error bars express SD with $n = 3$. Different letters above bars mean significant differences between treated cultures ($p < 0.05$, one-way ANOVA; Tukey's test).

Based on these results, we decided to investigate whether the uptake of radiolabeled precursors would also be blocked in the presence of terpenoids, as was the case with glucose. The uptake of precursors (thymidine, uridine, leucine, and N-acetyl glucosamine) was determined in the presence of celastrol, the triterpenoid that showed the greatest inhibitory effect on glucose uptake and macromolecular synthesis. Figure 5 shows how the addition of celastrol at 3 $\mu\text{g}/\text{mL}$ to *B. subtilis* cultures rapidly inhibited the uptake of [6- ^3H] thymidine and [5- ^3H] uridine by >50% between 2 and 5 min. The specific inhibitors of DNA and RNA synthesis, ciprofloxacin and rifampicin, did not affect the uptake of these precursors. The uptake of [4,5- ^3H] leucine was inhibited by up to 43% after 20 min, while uptake of N-acetyl-D-[1- ^{14}C] glucosamine was weakly affected and gradually increased during the experimentation time (Figure 5C,D). The addition of tetracycline blocked 75% the uptake of leucine in 10 min, whereas the transport of N-acetyl-D-[1- ^{14}C] glucosamine into the cells was not affected in the presence of penicillin.

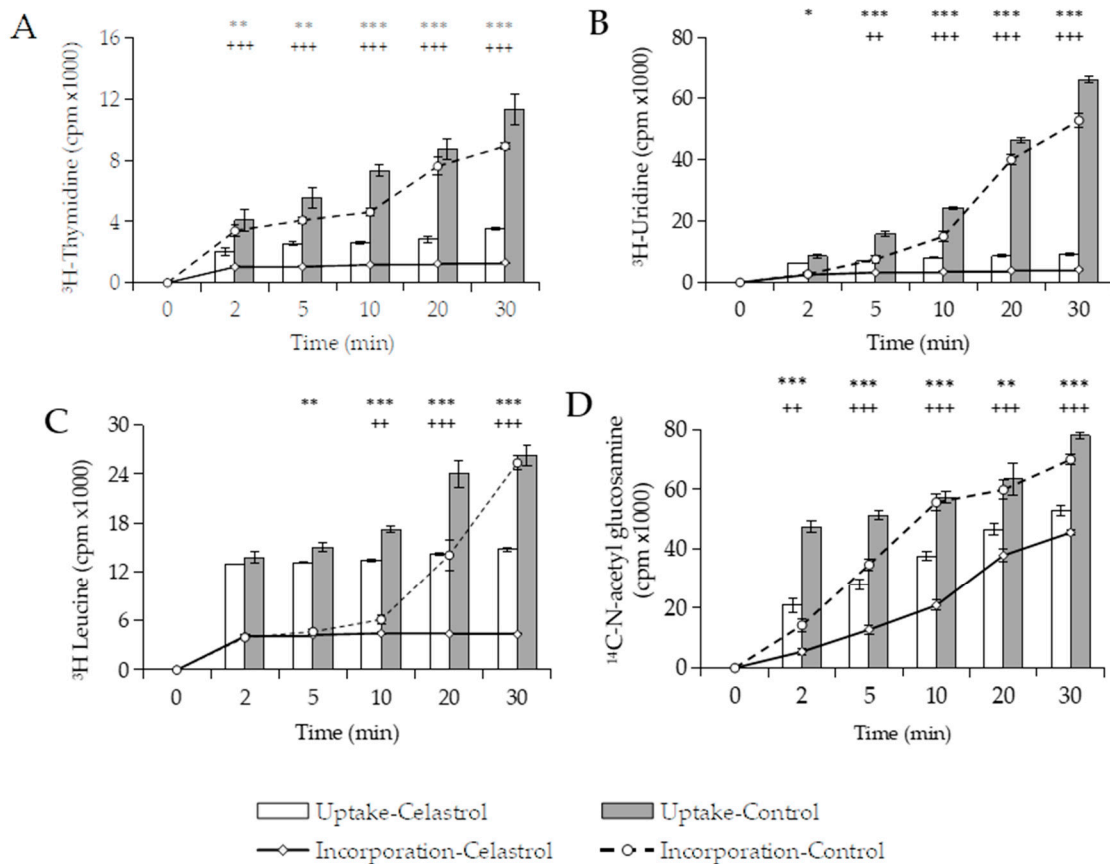


Figure 5. Incorporation (insoluble phase) and uptake (soluble phase) of DNA (A), RNA (B), protein (C), and cell wall (D) precursors on *B. subtilis* cultures in the presence of celastrol (3 µg/mL). Cultures in the same conditions but without celastrol and with the same proportion of DMSO were used as negative control. Error bars express SD with $n = 3$. Significant differences found in uptake (***: $p < 0.001$. **: $p < 0.01$. *: $p < 0.05$) or incorporation (+++: $p < 0.001$. ++: $p < 0.01$) compared with control (one-way ANOVA; Tukey's test).

Our results indicate that both uptake and incorporation processes in *B. subtilis* were affected by celastrol. Inhibition of macromolecular synthesis implies a low demand for biosynthetic precursors. Under these conditions, it would be reasonable to expect a slow-down in the uptake of precursors into the cell if both processes are coupled. In contrast, a primary blockage in precursor transport into the cells would also lead to inhibition of biosynthetic pathways due to low precursor availability. However, the uptake of precursors does not necessarily have to be linked to their incorporation in macromolecular synthesis. As Chou and Pogell [48] have previously suggested, if transport is inhibited and the process is not tightly coupled to macromolecular synthesis, the initial accumulation of precursors into the acid-soluble pool should be much more inhibited than their incorporation during macromolecular synthesis. In fact, these authors described how panamycin, an antibiotic that affects membrane-associated cellular functions, inhibits the uptake of uridine, while incorporation into biosynthetic processes is minimally affected. Thus, an ideal scenario would be one in which all of the precursors taken up by cells are in acid-soluble form to determine to what extent a blockage in molecular transport is a key process in the mechanism of action of the antibacterial agent [48].

Therefore, an experiment was conducted to investigate the effect of celastrol on the uptake of radiolabeled thymidine in *B. subtilis* when DNA synthesis was blocked by ciprofloxacin (1.25 µg/mL during 30 min). As seen in Figure 6, total radioactivity in control cells increased gradually throughout the incubation time. As expected, the incorporation of precursor slowed down when the biosynthetic process was specifically inhibited by ciprofloxacin. In this case, 5 min after the addition of the radiolabeled precursor, only ≈29%

of available thymidine was incorporated into macromolecular synthesis. By contrast, in the absence of ciprofloxacin, $\approx 74\%$ of the precursor present in the cells was incorporated in the same time (Figure 5A). This observation suggests that uptake and incorporation are independent processes and that the precursors can accumulate in the cytoplasm in the absence of incorporation. The addition of celastrol at $3 \mu\text{g/mL}$ not only blocked the uptake of thymidine radiolabeled precursor in the treated cells but also produced a slight leakage of accumulated $[6\text{-}^3\text{H}]$ thymidine from *B. subtilis*. This effect could be related to an action of celastrol on the integrity of the membrane, affecting its permeability and producing a release of the cytoplasmic content. Similar results have been observed on *S. aureus* cells treated with zeysterone, another triterpenoid with antibacterial properties, for which an action on the cytoplasmic membrane has also been suggested [49]. Additionally, the arrest of uptake was accompanied by an immediate blockage of incorporation into macromolecular synthesis. The results obtained reinforce the idea that celastrol could first target the function of the cytoplasmic membrane by affecting the transport of solutes and other essential molecules into the cell.

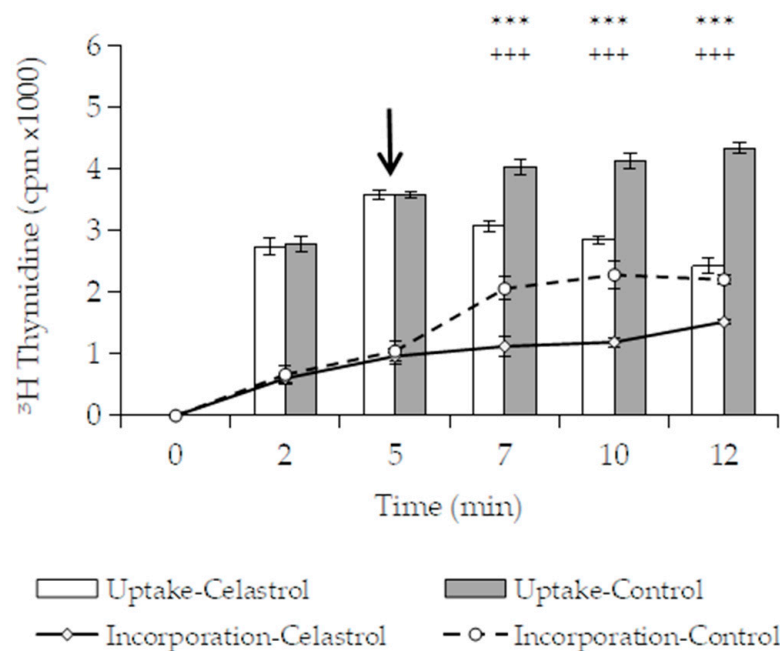


Figure 6. Incorporation (insoluble phase) and uptake (soluble phase) of radiolabeled ^3H -thymidine on *B. subtilis*. Bacterial culture were pretreated with ciprofloxacin ($1.25 \mu\text{g/mL}$), a specific inhibitors of DNA biosynthesis before the addition of the radiolabeled precursor (time 0). The triterpene celastrol ($3 \mu\text{g/mL}$), or the same proportion of DMSO used as control, was added at the time indicated by the arrow. Error bars express SD with $n = 3$. Significant differences found in uptake (***) or incorporation (+++) compared with control (one-way ANOVA; Tukey's test).

3.3.2. Effect of Celastrol on the Integrity and Functions of the Cytoplasmic Membrane

The cytoplasmic membrane is a delicate and metabolically active structure essential for the survival of microorganisms. It acts as a selective permeability barrier and prevents the loss of essential components of low molecular weight and nucleotide. Antibacterial agents targeting the cytoplasmic membrane affect its functions and cause a rapid release of low molecular weight compounds [50]. It has been described that the primary target site of the phenolic compounds in bacteria is the cytoplasmic membrane [51]. Damage to the cytoplasmic membrane impacts permeability barrier functions, which subsequently leads to a loss of structural integrity and a leakage of intracellular material. Thus, we also investigated the effect of celastrol on the cytoplasmic membrane of *B. subtilis* using (i) the BacLight test, (ii) detection of UV-absorbing material efflux, and (iii) determination of potassium leakage. Fluorescent dye and "LIVE/DEAD" BacLight Bacterial Viability Kits

have the capability of monitoring the viability of bacteria as a function of the cell membrane integrity [52,53]. Surprisingly, microscopic observations after the BacLight assay showed that the cells treated with celastrol maintained membrane integrity like the untreated cells. In contrast, cultures treated with clofocinol showed red fluorescence, an observation indicating membrane damage (Supplementary Materials Figure S1). When UV-absorbing material from *B. subtilis* cultures was monitored, concentrations up to 20 $\mu\text{g}/\text{mL}$ of celastrol did not alter the UV spectrum in comparison to the untreated cultures (Supplementary Materials Figure S2). Clofocinol used as a control clearly induced the release of UV-absorbing nucleotides in treated cells. Similar results were previously observed with netzahualcoyone, a terpenoid that interacts with the cytoplasmic membrane but also does not release materials that absorb at 260/280 nm [21]. We also determined the potassium released by *B. subtilis* cells as the first index of membrane damage [54]. Exposure to celastrol for 5 min induced intracellular potassium release compared with untreated cells, although the effect was significantly weaker than that observed with clofocinol (Figure 7). These data suggest that celastrol could act on biological membranes, altering their functions and modifying cell permeability.

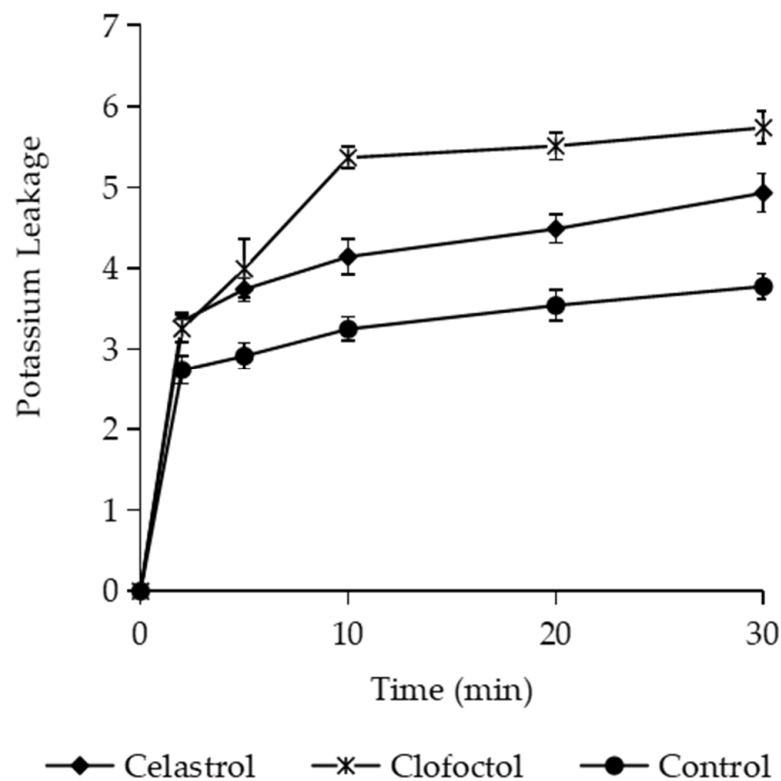


Figure 7. Potassium (K^+) leakage ($\mu\text{g}/\text{mL}$) from *Bacillus subtilis* cells exposed to celastrol (3 $\mu\text{g}/\text{mL}$). Cultures with clofocinol (5 $\mu\text{g}/\text{mL}$) or the maximum proportion of DMSO were used as positive and negative controls, respectively. Error bars express SD with $n = 3$.

3.3.3. Transmission Electron Microscopy

To determine whether celastrol induces noticeable cell membrane damage, transmission electron microscopy was performed on thin sections of *B. subtilis* treated with the terpenoid for 1 h. Compared to the untreated control, cells treated with celastrol exhibited abnormally long cells, variability in wall thickness, compact ribosomes underlying the plasma membrane, and mesosome-like structures arising from the septa (Figure 8).

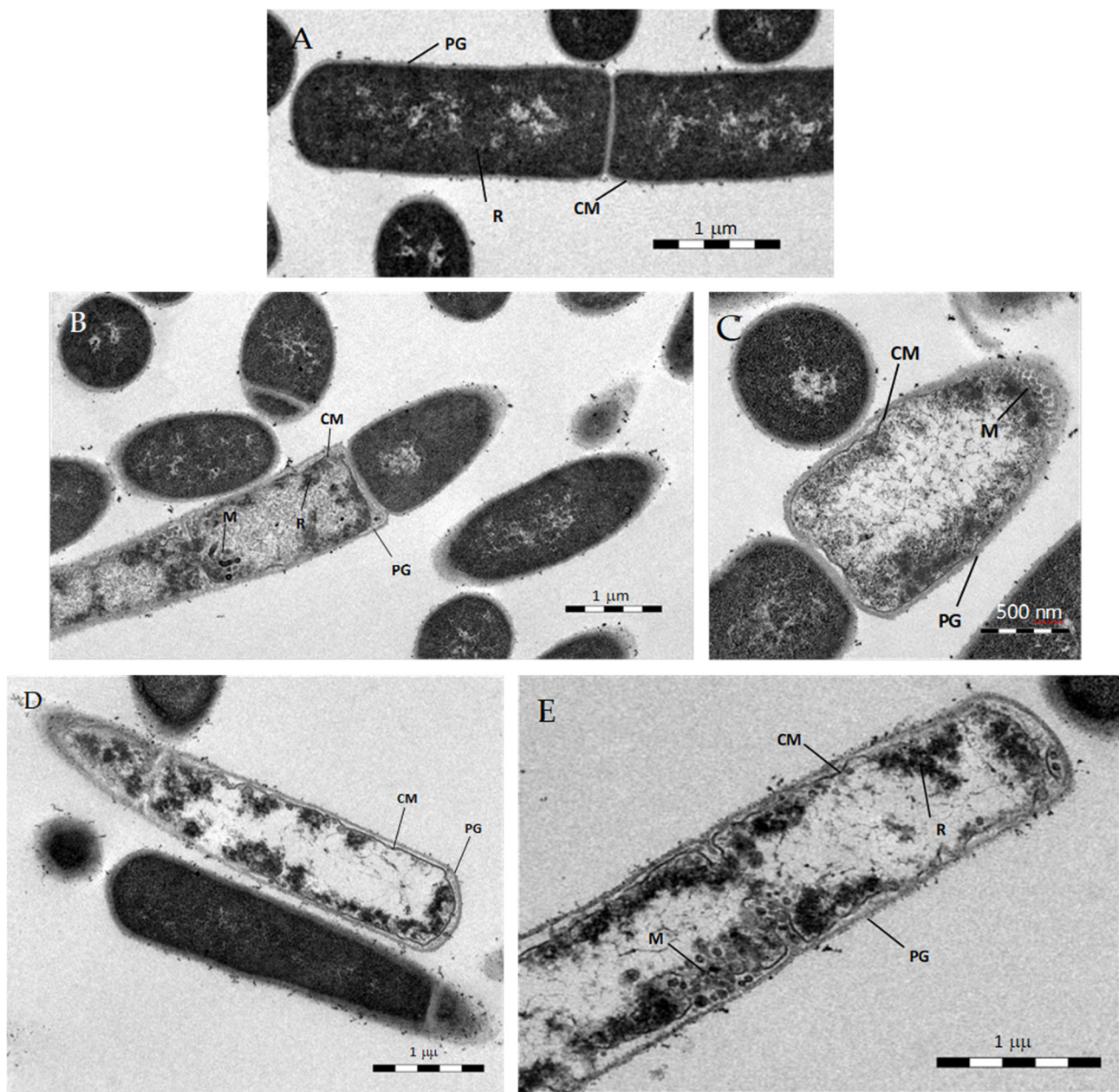


Figure 8. TEM of *B. subtilis* exposed for 1 h to celastrol at 3 µg/mL (B,C) or pristimerin at 10 µg/mL (D,E). Untreated cells (A). CM, cytoplasmic membrane; PG, peptidoglycan layer; R, ribosomes; M, mesosome-like structures.

Despite the multiple effects produced by celastrol, the technique did not allow the observation of visible damage to the cell membrane. For comparison purposes, *B. subtilis* treated with pristimerin at 10 µg/mL, which showed a bacteriolytic effect during killing curves assays, was also observed. As with celastrol, the cells were extremely long, spindle-shaped, with thin cell walls and slightly electron-dense cytoplasm with ribosomes associated to the inner face of the membrane (Figure 8D,E). These observations resemble those obtained by da Cruz et al. [42] on cultures of *S. aureus* treated with pristimerin, where the cells presented a disrupted membrane, as well as a loss of cell integrity.

3.3.4. Effect of Celastrol on Cellular Respiration

Another fundamental function of the cytoplasmic membrane is cellular respiration. The respiratory chain plays an important role in the energetic metabolism of a cell, the maintenance of intracellular redox balance, or the protection against oxidative stress [55].

The membranes harbor the electron transport chain, a well-known system with oxygen as the final electron acceptor in aerobic respiration processes.

Thus, the effect of celastrol on oxygen consumption was also evaluated on cell cultures of *B. subtilis* and *E. coli*, as well as in acellular preparations of these bacteria obtained by cell disruption. Table 3 summarizes the results of the effect of celastrol on glucose-dependent oxygen uptake in intact cells of *B. subtilis* and *E. coli*. Both celastrol and NaCN produced an immediate inhibition of oxygen consumption in *B. subtilis*, reaching 60% at 8 min after their addition compared to the untreated control. As expected, celastrol barely affected the oxygen uptake in *E. coli*, as Gram-negative bacteria are insensitive to the terpene quinone.

Table 3. Mean values \pm standard deviations of means ($n = 3$) of oxygen consumption rates ($\mu\text{L O}_2/\text{min}$) at different times in whole cells or membrane preparations of *B. subtilis* and *E. coli* without treatment or after treatments with celastrol at $3 \mu\text{g}/\text{mL}$ or sodium cyanide (NaCN) at 6.7 mM used as positive controls. The percentage (%) of inhibition in the oxygen consumption referring to the untreated cells (negative control) is shown in parentheses.

Bacteria	Time (min)	Oxygen Consumption ¹					
		Whole Cells (Glucose 1%)			Membrane Fraction (NADH 0.1 mM)		
		Control	NaCN	Celastrol	Control	NaCN	Celastrol
<i>B. subtilis</i>	0	2.36 \pm 0.10 ^a	2.30 \pm 0.07 ^a (2.4%)	2.27 \pm 0.12 ^a (3.9%)	0.54 \pm 0.05 ^a	0.50 \pm 0.06 ^a (6.9%)	0.52 \pm 0.08 ^a (4.0%)
	2	3.69 \pm 0.17 ^a	2.71 \pm 0.05 ^b (26.5%)	2.74 \pm 0.15 ^b (25.7%)	0.98 \pm 0.11 ^a	0.66 \pm 0.00 ^b (31.7%)	0.68 \pm 0.01 ^b (30.6%)
	4	5.42 \pm 0.46 ^a	2.77 \pm 0.08 ^b (48.6%)	3.11 \pm 0.04 ^b (42.4%)	1.27 \pm 0.01 ^a	0.79 \pm 0.00 ^c (37.7%)	0.82 \pm 0.02 ^b (35.1%)
	6	7.09 \pm 0.21 ^a	2.91 \pm 0.03 ^c (58.9%)	3.30 \pm 0.02 ^b (53.5%)	1.56 \pm 0.05 ^a	0.89 \pm 0.01 ^b (43.0%)	0.94 \pm 0.03 ^b (39.4%)
	8	8.53 \pm 0.14 ^a	2.97 \pm 0.02 ^c (65.2%)	3.42 \pm 0.04 ^b (59.8%)	1.80 \pm 0.01 ^a	0.94 \pm 0.00 ^c (47.9%)	1.01 \pm 0.02 ^b (43.9%)
<i>E. coli</i>	0	2.16 \pm 0.07 ^a	2.04 \pm 0.06 ^{ab} (5.5%)	2.00 \pm 0.02 ^b (7.3%)	2.22 \pm 0.07 ^a	2.10 \pm 0.01 ^{ab} (5.0%)	2.07 \pm 0.05 ^b (6.5%)
	2	3.35 \pm 0.14 ^a	2.16 \pm 0.03 ^c (35.5%)	3.08 \pm 0.08 ^b (7.9%)	3.07 \pm 0.00 ^a	2.20 \pm 0.05 ^c (28.2%)	2.41 \pm 0.02 ^b (21.3%)
	4	4.34 \pm 0.24 ^a	2.22 \pm 0.03 ^b (48.8%)	3.95 \pm 0.14 ^a (9.0%)	3.88 \pm 0.01 ^a	2.30 \pm 0.03 ^c (40.6%)	2.51 \pm 0.01 ^b (35.3%)
	6	5.80 \pm 0.32 ^a	2.32 \pm 0.03 ^c (60.0%)	4.84 \pm 0.10 ^b (16.6%)	4.74 \pm 0.01 ^a	2.34 \pm 0.02 ^c (50.6%)	2.61 \pm 0.02 ^b (44.9%)
	8	6.79 \pm 0.19 ^a	2.40 \pm 0.05 ^c (64.6.4%)	5.53 \pm 0.09 ^b (18.5%)	5.37 \pm 0.00 ^a	2.40 \pm 0.08 ^c (55.3%)	2.68 \pm 0.01 ^b (50.0%)

¹ For each assessment, values with different superscript letters within each given time point indicate statistically significant differences (ANOVA, Tukey's multiple comparison test, $p < 0.05$).

The same evaluation was carried out on acellular preparations where the oxygen consumption was coupled to the oxidation of NADH. Unlike when whole cells were used, here, NADH oxidation only depended on the amount of dissolved oxygen and the function of the respiratory chain. In these conditions, the addition of celastrol and NaCN inhibited the oxygen consumption in *B. subtilis* and *E. coli* preparations. The different behavior shown by celastrol in intact and disrupted preparations of *E. coli* cells shows that the cell membranes of both Gram-positive and -negative bacteria are equally sensitive to its action. The outer membranes of Gram-negative bacteria act as a permeability barrier, holding celastrol physically distant from its target of action. These results indicate that celastrol has a direct effect on the electron transport chain, affecting the consumption of oxygen and, consequently, the oxidation of NADH associated with respiration processes. However, in the presence of celastrol, neither a spontaneous oxidation of NADH nor a reduction in NAD^+ was observed.

An additional experiment was carried out to verify previous results indicating an action of celastrol on the inhibition of enzymatic activity. Nagase et al. [56] reported that celastrol can inhibit topoisomerase II and trigger apoptosis in HL-60 cells. DNA gyrase is an important bacterial topoisomerase II that catalyzes ATP-dependent negative supercoiling

of bacterial DNA. The essential role of gyrase is to maintain the topological constitution of DNA and, hence, the survival of bacteria [57]. Eukaryotic cells lack the enzyme, which has led to the development of specific antimicrobials targeting the gyrase functions [58]. Our results confirmed the effect of celastrol at 50 µg/mL on the gyrase activity of supercoiling plasmid pBR322, as did ciprofloxacin, used as a positive control (Supplementary Materials Figure S3). Interestingly, pristimerin has shown a weaker antibacterial action compared to celastrol and did not affect the enzymatic activity of gyrase. This mechanism of action has been suggested for other triterpenoid compounds showing activity against topoisomerases I and II [59]. Some models have been proposed for the mode of action of triterpenoids on topoisomerases, which can be either by binding to the enzyme at the DNA binding site or by binding to the ATP binding site, conformationally blocking DNA binding to the enzyme [60]. Thus, the effect on DNA supercoiling produced by celastrol could be related with an action on the gyrase rather than a direct DNA binding effect.

4. Conclusions

The antimicrobial action of celastrol and pristimerin, two natural triterpene methylene quinones, was evaluated, and the mechanism of action against the spore-forming bacteria *Bacillus subtilis* was also approached. Celastrol showed a higher antimicrobial effect compared with pristimerin, being active against Gram-positive bacteria. The results obtained in this study indicate that celastrol interacts with the cytoplasmic membrane of *B. subtilis*, preventing the transport of solutes into the cells and affecting basic membrane functions such as respiration processes. At the structural level, the membrane was not widely affected, suggesting a mechanism of action for celastrol other than a simple effect on structural components and subsequent membrane disruption. Furthermore, celastrol can also interact with enzymatic processes different from those exclusively located on the cytoplasmic membrane, as observed here for topoisomerase II. Although further investigations are required to elucidate a more precise mechanism of action, our results indicate that celastrol can act on multiple targets.

Supplementary Materials: The following are available online at <https://www.mdpi.com/2304-8158/10/3/591/s1>, Figure S1: Epifluorescence microscopy images of *B. subtilis* stained with propidium iodide and SYTO 9 after treatment with celastrol (3 µg/mL) for 30 and 60 min (A,B) or clofoctol (5 µg/mL) for 30 min (C). Control cells were treated with the maximum proportion of DMSO (D). Scale bars correspond to 10 µm. Figure S2: Release of 260 and 280 nm absorbing material from *B. subtilis* cells treated with celastrol at 3, 6, and 10 µg/mL and clofoctol at 5 µg/mL. Cells exposed to the maximum proportion of DMSO were used as control. Error bars express SD with $n = 3$. Figure S3: DNA supercoiling assays. Electrophoresis gel shows a control with a negatively supercoiled plasmid (line 1) with DMSO (line 2), and after its treatment with ciprofloxacin at 25 (line 3) and 50 µg/mL (line 4), celastrol at 50 µg/mL (line 5), and pristimerin at 50 µg/mL (line 6).

Author Contributions: Conceptualization, L.M. and L.d.L.G.; methodology, L.M. and L.d.L.G.; investigation, N.P.-M. and L.d.L.G.; data curation, L.M., N.P.-M. and L.d.L.G.; writing—original draft preparation, L.M. and L.d.L.G.; writing—review and editing, L.M. and L.d.L.G.; supervision, L.M. and L.d.L.G.; funding acquisition, L.M. All authors have read and agreed to the published version of the manuscript.

Funding: This study was supported by RTI2018-094356-B-C21 Spanish Ministerio de Economía, Industria y Competitividad (MINECO) and co-funded by the European Regional Development Fund (FEDER) projects.

Institutional Review Board Statement: Not applicable.

Informed Consent Statement: Not applicable.

Data Availability Statement: Not applicable.

Acknowledgments: Thanks are due to the Universidad de La Laguna and Servicio de Microscopia de la Universidad de Las Palmas de Gran Canaria.

Conflicts of Interest: The authors declare no conflict of interest.

References

1. González, A.G.; Bazzocchi, I.L.; Moujir, L.; Jiménez, I.A. Ethnobotanical uses of Celastraceae. Bioactive metabolites. In *Studies in Natural Products Chemistry: Bioactive Natural Products (Part D)*; Atta-ur, R., Ed.; Elsevier Science Publisher: Amsterdam, The Netherlands, 2000; Volume 23, pp. 649–738.
2. Simmons, M.P.; Cappa, J.J.; Archer, R.H.; Ford, A.J.; Eichstedt, D.; Clevinger, C.C. Phylogeny of the Celastreae (Celastraceae) and the relationships of *Catha edulis* (qat) inferred from morphological characters and nuclear and plastid genes. *Mol. Phylogenet. Evol.* **2008**, *48*, 745–757. [[CrossRef](#)] [[PubMed](#)]
3. Gunatilaka, A.A.L. Triterpenoid Quinonemethides and Related Compounds (celastroloids). In *Progress in the Chemistry of Organic Natural Products*; Herz, W., Kirby, G.W., Moore, R.E., Steglich, W., Tamm, C., Eds.; Springer: New York, NY, USA, 1996; Volume 67, pp. 1–123.
4. Bashir, A.Y.; Hozeifa, M.H.; Zhang, L.-Y.; Jiang, Z.-Z. Anticancer Potential and Molecular Targets of Pristimerin: A Mini-Review. *Curr. Cancer Drugs Targets* **2017**, *17*, 100–108. [[CrossRef](#)]
5. Hou, W.; Liu, B.; Xu, H. Celastrol: Progresses in structure-modifications, structure-activity relationships, pharmacology and toxicology. *Eur. J. Med. Chem.* **2020**, *189*, 112081. [[CrossRef](#)]
6. El-Agamy, D.S.; Shaaban, A.A.; Almaramhy, H.H.; Elkablawy, S.; Elkablawy, M.A. Pristimerin as a Novel Hepatoprotective Agent against Experimental Autoimmune Hepatitis. *Front. Pharmacol.* **2018**, *9*, 292. [[CrossRef](#)] [[PubMed](#)]
7. Venkatesha, S.H.; Moudgil, K.D. Celastrol and Its Role in Controlling Chronic Diseases. *Adv. Exp. Med. Biol.* **2016**, *928*, 267–289. [[CrossRef](#)]
8. Shi, J.; Li, J.; Xu, Z.; Chen, L.; Luo, R.; Zhang, C.; Gao, F.; Zhang, J.; Fu, C. Celastrol: A Review of Useful Strategies Overcoming its Limitation in Anticancer Application. *Front. Pharmacol.* **2020**, *11*, 558741. [[CrossRef](#)] [[PubMed](#)]
9. Cascão, R.; Fonseca, J.E.; Moita, L.F. Celastrol: A Spectrum of Treatment Opportunities in Chronic Diseases. *Front. Med.* **2017**, *4*, 69. [[CrossRef](#)]
10. Kashyap, D.; Sharma, A.; Tuli, H.S.; Sak, K.; Mukherjee, T.; Bishayee, A. Molecular targets of celastrol in cancer: Recent trends and advancements. *Crit. Rev. Oncol. Hematol.* **2018**, *128*, 70–81. [[CrossRef](#)]
11. Lan, G.; Zhang, J.; Ye, W.; Yang, F.; Li, A.; He, W.; Zhang, W.D. Celastrol as a tool for the study of the biological events of metabolic diseases. *Sci. China Chem.* **2019**, *62*, 409–416. [[CrossRef](#)]
12. Liu, J.; Lee, J.; Salazar Hernandez, M.A.; Mazitschek, R.; Ozcan, U. Treatment of Obesity with Celastrol. *Cell* **2015**, *161*, 999–1011. [[CrossRef](#)] [[PubMed](#)]
13. Pfuhlmann, K.; Schriever, S.C.; Baumann, P.; Kabra, D.G.; Harrison, L.; Mazibuko-Mbeje, S.E.; Contreras, R.E.; Kyriakou, E.; Simonds, S.E.; Tiganis, T.; et al. Celastrol-Induced Weight Loss Is Driven by Hypophagia and Independent From UCP1. *Diabetes* **2018**, *7*, 2456–2465. [[CrossRef](#)] [[PubMed](#)]
14. Moujir, L.; Gutiérrez-Navarro, A.M.; González, A.G.; Ravelo, A.G.; Luis, J.G. The relationship between structure and antimicrobial activity in quinones from the Celastraceae. *Biochem. Syst. Ecol.* **1990**, *18*, 25–28. [[CrossRef](#)]
15. Sotanaphun, U.; Lipipun, V.; Suttisri, R.; Bavovada, R. Antimicrobial activity and stability of tingenone derivatives. *Planta Med.* **1999**, *65*, 450–452. [[CrossRef](#)]
16. Moujir, L.; Gutiérrez-Navarro, A.M.; González, A.G.; Ravelo, A.G.; Luis, J.G. Mode of action of netzahualcoyone. *Antimicrob. Agents Chemother.* **1991**, *35*, 211–213. [[CrossRef](#)] [[PubMed](#)]
17. De León, L.; Moujir, L. Activity and mechanism of the action of zeylasterone against *B. subtilis*. *J. Appl. Microbiol.* **2007**, *104*, 1266–1274. [[CrossRef](#)] [[PubMed](#)]
18. Woo, S.-G.; Lee, A.-Y.; Lee, S.-M.; Lim, K.-H.; Ha, E.-J.; Eom, Y.-B. Activity of novel inhibitors of *Staphylococcus aureus* biofilms. *Folia Microbiol.* **2017**, *62*, 157–167. [[CrossRef](#)]
19. Ooi, N.; Eady, E.A.; Cove, J.H.; O'Neill, A.J. Redox-active compounds with a history of human use: Antistaphylococcal action and potential for repurposing as topical antibiofilm agents. *J. Antimicrob. Chemother.* **2015**, *70*, 479–488. [[CrossRef](#)] [[PubMed](#)]
20. Kim, H.-R.; Lee, D.; Eom, Y.-B. Anti-biofilm and Anti-Virulence Efficacy of Celastrol against *Stenotrophomonas maltophilia*. *Int. J. Med. Sci.* **2018**, *15*, 617–627. [[CrossRef](#)] [[PubMed](#)]
21. Pérez, M.; Sánchez, M.; Stupak, M.; García, M.; Rojo de Almeida, M.T.; Oberti, J.C.; Palermo, J.; Blustein, G. Antifouling Activity of Celastroids Isolated from *Maytenus* Species, Natural and Sustainable Alternatives for Marine Coatings. *Ind. Eng. Chem. Res.* **2014**, *53*, 7655–7659. [[CrossRef](#)]
22. Luo, D.Q.; Wang, H.; Tian, X.; Shao, H.J.; Liu, J.K. Antifungal properties of pristimerin and celastrol isolated from *Celastrus hypoleucus*. *Pest Manag. Sci.* **2005**, *61*, 85–90. [[CrossRef](#)]
23. Gullo, F.P.; Sardi, J.C.; Santos, V.A.; Sangalli-Leite, F.; Pitanguí, N.S.; Rossi, S.A.; de Paula, E.; Silva, A.C.; Soares, L.A.; Silva, J.F.; et al. Antifungal activity of maytenin and pristimerin. *Evid. Based Complement. Alternat. Med.* **2012**, *2012*, 340787. [[CrossRef](#)]
24. Haque, E.; Irfan, S.; Kamil, M.; Sheikh, S.; Hasan, A.; Ahmad, A.; Lakshmi, V.; Nazir, A.; Mir, S.S. Terpenoids with antifungal activity trigger mitochondrial dysfunction in *Saccharomyces cerevisiae*. *Microbiology* **2016**, *85*, 436–443. [[CrossRef](#)]
25. Song, J.; Shang, N.; Baig, N.; Yao, J.; Shin, C.; Kim, B.K.; Li, Q.; Malwal, S.R.; Oldfield, E.; Feng, X.; et al. *Aspergillus flavus* squalene synthase as an antifungal target: Expression, activity, and inhibition. *Biochem. Biophys. Res. Commun.* **2019**, *512*, 517–523. [[CrossRef](#)]

26. Seo, W.-D.; Lee, D.-Y.; Park, K.H.; Kim, J.-H. Downregulation of fungal cytochrome c peroxidase expression by antifungal quinonemethide triterpenoids. *Appl. Biol. Chem.* **2016**, *59*, 281–284. [[CrossRef](#)]
27. Sun, Q.; Li, C.; Jing, L.; Peng, X.; Wang, Q.; Jiang, N.; Xu, Q.; Zhao, G. Celastrol ameliorates *Aspergillus fumigatus* keratitis via inhibiting LOX-1. *Int. Immunopharmacol.* **2019**, *70*, 101–109. [[CrossRef](#)] [[PubMed](#)]
28. Tseng, C.-K.; Hsu, S.-P.; Lin, C.-K.; Wu, Y.-H.; Lee, J.-C.; Young, K.-C. Celastrol inhibits hepatitis C virus replication by upregulating heme oxygenase-1 via the JNK MAPK/Nrf2 pathway in human hepatoma cells. *Antiviral. Res.* **2017**, *146*, 191–200. [[CrossRef](#)] [[PubMed](#)]
29. Zhang, H.; Lu, G. Synthesis of celastrol derivatives as potential non-nucleoside hepatitis B virus inhibitors. *Chem. Biol. Drug Des.* **2020**, *96*, 1380–1386. [[CrossRef](#)]
30. Kumar, T.D.K.; Murali, H.S.; Batra, H.V. Simultaneous detection of pathogenic *B. cereus*, *S. aureus* and *L. monocytogenes* by multiplex PCR. *Indian J. Microbiol.* **2009**, *49*, 283–289. [[CrossRef](#)]
31. Kubo, I.; Fujita, K.-I.; Nihei, K.-I.; Nihei, A. Antibacterial Activity of Akyl Gallates against *Bacillus subtilis*. *J. Agric. Food Chem.* **2004**, *52*, 1072–1076. [[CrossRef](#)]
32. Gopal, N.; Hill, C.; Ross, P.R.; Beresford, T.P.; Fenelon, M.A.; Cotter, P.D. The Prevalence and Control of *Bacillus* and Related Spore-Forming Bacteria in the Dairy Industry. *Front. Microbiol.* **2015**, *6*, 1418. [[CrossRef](#)]
33. Gaur, A.H.; Patrick, C.C.; McCullers, J.A.; Flynn, P.M.; Pearson, T.A.; Razzouk, B.I.; Thompson, S.J.; Shenep, J.L. *Bacillus cereus* Bacteremia and Meningitis in Immunocompromised Children. *Clin. Infect. Dis.* **2001**, *32*, 1456–1462. [[CrossRef](#)] [[PubMed](#)]
34. Dabscheck, G.; Silverman, L.; Ullrich, N.J. *Bacillus cereus* Cerebral Abscess during Induction Chemotherapy for Childhood Acute Leukemia. *J. Pediatr. Hematol. Oncol.* **2015**, *37*, 568–569. [[CrossRef](#)]
35. Hansford, J.R.; Phillips, M.; Cole, C.; Francis, J.; Blyth, C.C.; Gottardo, N.G. *Bacillus cereus* bacteremia and multiple brain abscesses during acute lymphoblastic leukemia induction therapy. *J. Pediatr. Hematol. Oncol.* **2014**, *36*, e197–e201. [[CrossRef](#)] [[PubMed](#)]
36. Cowan, M.M. Plant Products as Antimicrobial Agents. *Clin. Microbiol. Rev.* **1999**, *12*, 564–582. [[CrossRef](#)]
37. Nuñez, M.J.; Kennedy, M.L.; Jiménez, I.A.; Bazzocchi, I.L. Uragogin and blepharodin, unprecedented hetero-Diels-Alder adducts from Celastraceae species. *Tetrahedron* **2011**, *67*, 3030–3033. [[CrossRef](#)]
38. Taddeo, V.A.; Castillo, U.C.; Martínez, M.L.; Menjivar, J.; Jimenez, I.A.; Nunez, M.J.; Bazzochi, I.L. Development and validation of an HPLC-PDA method for biologically active quinonemethide triterpenoids isolated from *Maytenus chiapensis*. *Medicines* **2019**, *6*, 36. [[CrossRef](#)]
39. Clinical and Laboratory Standards Institute (CLSI; formerly NCCLS); National Committee for Clinical Laboratory Standards. *Performance Standards for Antimicrobial Susceptibility Testing*; 16th Informational Supplement; CLSI Document M7-A7; Clinical and Laboratory Standards Institute: Wayne, PA, USA, 2006. Available online: <https://clsi.org/> (accessed on 10 March 2021).
40. CLSI. *Methods for Dilution Antimicrobial Susceptibility Tests for Bacteria that Grow Aerobically*; Approved Standard, 9th ed.; CLSI Document M07-A9; Clinical and Laboratory Standards Institute: Wayne, PA, USA, 2012.
41. Davis, B.D.; Mignoli, E.S. Mutants of *Escherichia coli* requiring methionine or vitamin B₁₂. *J. Bacteriol.* **1950**, *60*, 17–28. [[CrossRef](#)]
42. Da Cruz Nizer, W.S.; Ferraz, A.C.; Moraes, T.F.S.; Lima, W.G.; Santos, J.P.; Duarte, L.P.; Ferreira, J.M.S.; de Brito Magalhães, C.L.; Vieira-Filho, S.A.; dos Santos PereiraAndrade, A.C.; et al. Pristimerin isolated from *Salacia crassifolia* (Mart. Ex. Schult.) G. Don. (Celastraceae) roots as a potential antibacterial agent against *Staphylococcus aureus*. *J. Ethnopharmacol.* **2021**, *266*, 113423. [[CrossRef](#)] [[PubMed](#)]
43. Moujir, L.; López, M.R.; Reyes, C.P.; Jiménez, I.A.; Bazzocchi, I.L. Structural requirements from antimicrobial activity of phenolic nor-triterpenes from Celastraceae species. *Appl. Sci.* **2019**, *9*, 2957. [[CrossRef](#)]
44. He, Q.-W.; Feng, J.-H.; Hu, X.-L.; Long, H.; Huang, X.-F.; Jiang, Z.Z.; Zhang, X.-Q.; Ye, W.-C.; Wang, H. Synthesis and Biological Evaluation of Celastrol Derivatives as Potential Immunosuppressive Agents. *J. Nat. Prod.* **2020**, *83*, 2578–2586. [[CrossRef](#)]
45. Yablonsky, F. Alteration of Membrane Permeability in *Bacillus subtilis* by Clofoctol. *J. Gen. Microbiol.* **1983**, *129*, 1089–1195. [[CrossRef](#)]
46. Oliva, B.; Miller, K.; Caggiano, N.; O’neill, A.J.; Cuny, G.D.; Hoemarm, M.Z.; Hauske, J.R.; Chopra, I. Biological properties of novel antistaphylococcal quinoline-indole agents. *Antimicrob. Agents Chemother.* **2003**, *47*, 458–466. [[CrossRef](#)]
47. Wang, C.-M.; Jhan, Y.-L.; Tsai, S.-J.; Chou, C.-H. The Pleiotropic Antibacterial Mechanisms of Ursolic Acid against Methicillin-Resistant *Staphylococcus aureus* (MRSA). *Molecules* **2016**, *21*, 884. [[CrossRef](#)] [[PubMed](#)]
48. Chou, W.-G.; Pogell, B.M. Mode of Action of Pamamycin in *Staphylococcus aureus*. *Antimicrob. Agents Chemother.* **1981**, *20*, 443–454. [[CrossRef](#)] [[PubMed](#)]
49. De León, L.; López, M.R.; Moujir, L. Antibacterial properties of zeylasterone, a triterpenoid isolated from *Maytenus blepharodes*, against *Staphylococcus aureus*. *Microbiol. Res.* **2010**, *165*, 617–626. [[CrossRef](#)]
50. Epand, R.M.; Walker, C.; Epand, R.F.; Magarvey, N.A. Molecular mechanisms of membrane targeting antibiotics. *Biochim. Biophys. Acta* **2016**, *1858*, 980–987. [[CrossRef](#)]
51. Rempe, C.S.; Burris, K.P.; Lenaghan, S.C.; Stewart, C.N. The Potential of Systems Biology to Discover Antibacterial Mechanisms of Plant Phenolics. *Front. Microbiol.* **2017**, *8*, 422. [[CrossRef](#)] [[PubMed](#)]
52. Bunthof, C.J.; Van Schalkwijk, S.; Meijer, W.; Abee, T.; Hugenholtz, J. Fluorescent method for monitoring cheese starter permeabilization and lysis. *Appl. Environ. Microbiol.* **2001**, *67*, 4264–4271. [[CrossRef](#)]
53. Laflamme, C.; Lavigne, S.; Ho, J.; Duchaine, C. Assessment of bacterial endospore viability with fluorescent dyes. *J. Appl. Microbiol.* **2004**, *96*, 684–692. [[CrossRef](#)]

54. Lambert, P.A.; Hammond, S.M. Potassium fluxes, first indications of membrane damage in micro-organisms. *Biochem. Biophys. Res. Commun.* **1973**, *18*, 796–799. [[CrossRef](#)]
55. Kalnenieks, U.; Balodite, E.; Rutkis, R. Metabolic Engineering of Bacterial Respiration: High vs. Low P/O and the Case of *Zymomonas mobilis*. *Front. Bioeng. Biotechnol.* **2019**, *7*, 327. [[CrossRef](#)] [[PubMed](#)]
56. Nagase, M.; Oto, J.; Sugiyama, S.; Yube, K.; Takaishi, Y.; Sakato, N. Apoptosis Induction in HL-60 Cells and Inhibition of Topoisomerase II by Triterpene Celastrol. *Biosci. Biotechnol. Biochem.* **2003**, *67*, 1883–1887. [[CrossRef](#)]
57. Kolarič, A.; Anderluh, M.; Minovski, N. Two Decades of Successful SAR-Grounded Stories of the Novel Bacterial Topoisomerase Inhibitors (NBTIs). *J. Med. Chem.* **2020**, *63*, 5664–5674. [[CrossRef](#)] [[PubMed](#)]
58. D’Atanasio, N.; Capezzone de Joannon, A.; Di Sante, L.; Mangano, G.; Ombrato, R.; Vitiello, M.; Bartella, C.; Magarò, G.; Prati, F.; Milanese, C.; et al. Antibacterial activity of novel dual bacterial DNA type II topoisomerase inhibitors. *PLoS ONE* **2020**, *15*, e0228509. [[CrossRef](#)] [[PubMed](#)]
59. D’yakonov, V.A.; Dzhemileva, L.U.; Dzhemilev, U.M. Advances in the chemistry of natural and semisynthetic topoisomerase I/II inhibitors. In *Studied Natural Products Chemistry*; Atta-ur-Rahman, F., Ed.; Elsevier Science Publisher: Amsterdam, The Netherlands, 2017; Volume 54, pp. 21–86. [[CrossRef](#)]
60. Setzer, W.N. Non-Intercalative Triterpenoid Inhibitors of Topoisomerase II: A Molecular Docking Study. *Open Bioact. Compd. J.* **2008**, *1*, 13–17. [[CrossRef](#)]